Development of single sensor fast response pressure probes

Keizo Tanaka[1*], *Anestis I.* Kalfas[2†], and *Howard P.* Hodson[2‡]

[1]Mitsubishi Heavy Industries, Takasago, Japan
[2]Cambridge University, Engineering Department, Whittle Laboratory, Madingley Road, Cambridge CB3 0DY, England

Abstract. Multi-sensor fast response pressure probes are often used in turbomachinery investigations. However, the size of multi-sensor probes are often larger than is ideal. This paper describes the development of a single sensor pressure probe that has sufficient sensitivity for the measurements of unsteady 3D flow fields in turbomachines. Because there is only one sensor, the probe can be made much smaller than previous designs. Several types of probe were designed and tested using largescale models in a wind tunnel. Both the steady state and the dynamic response have been investigated. The relationship between the shape of the probe and its yaw and pitch sensitivity has been investigated through measurements of the pressure distribution on the large-scale models and through visualizations of the flow. Dambach and Hodson [3] proposed a new method of data reduction for a single sensor pressure probe. In that work, a single sensor pressure probe with the shape of a triangular prism was fabricated and tested with success in a radial flow turbine where the flow field was mainly 2D. The probe was shown to have only yaw sensitivity while pitch sensitivity is also important in the survey of three dimensional turbomachinery flows. In this paper, the model probes were used to assess the pitch sensitivity of single sensor pressure probes. All the probes have the sensing face at the end of a radially mounted stem so that they can be used for inter bladerow measurements. Through the steady state measurements, the dependency of pitch sensitivity on (1) the shape of the probe stem (e.g., Square, Circular, and Triangular) and (2) the angle of the slanted sensing face at the tip of the probe were investigated. Having assessed all the designs based on the steady state experiments, the dynamic behaviour of selected designs was investigated. The results indicate that a slanted face and appropriate probe tip design can be used to increase the pitch sensitivity of the single sensor probe to acceptable levels.

Nomenclature

Re	Reynolds Number
St	Strouhal Number
N	number of orientation
P	pressure
S	pitch sensitivity
V	velocity
f	frequency
d	diameter of probes
C_p	pressure coefficient $(=(P-P_s)/(P_t-P_s))$
α	yaw angle
β	pitch angle
$C_p(\alpha,\beta)$	C_p at yaw angle of α and pitch angle β
ρ	density

Sub- and Superscripts

s	static
d	dynamic
t	total
cal	calibration
y	yaw
p	pitch
abs	absolute
rel	relative
i,j	index
*	non-dimensional value

* *Keizo* Tanaka: keizo_tanaka@mhi.co.jp
† *Anestis I.* Kalfas: akalfas@auth.gr
‡ *Howard P.* Hodson: hph@eng.cam.ac.uk

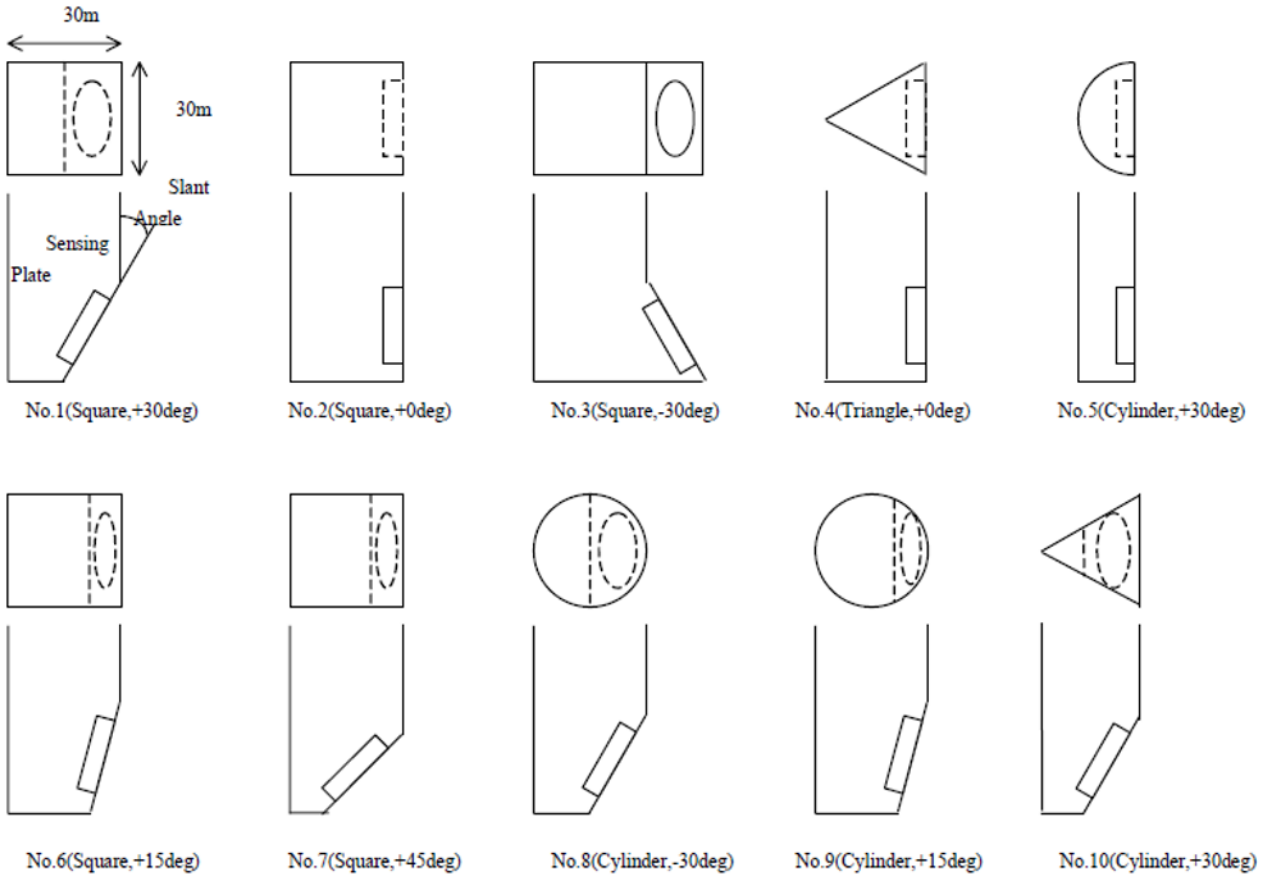

Fig. 1. Probe geometries tested

1 Introduction

A number of types of probes have been used in turbomachinery investigations. Many investigators have employed single sensor hot wire anemometers in multiple positions to determine the mean velocity vector, turbulence intensities and Reynolds stresses. Likewise, investigators have used multi-sensor fast response pressure probes to measure an unsteady flow field. Unfortunately, they are often larger than is ideal (e.g. 2.5 to 6 mm; see Grossweiler et al [6], Cherret et al [2]) for many facilities. While these probes may provide data of acceptable quality in relatively large-scale facilities, such facilities are rare. On the other hand, single sensor pressure probes can be typically made to be a half to a third of the size of multi-sensor probes. Furthermore, because a single sensor is employed, the calibration is simpler and changes in calibration due to ambient changes are easier to accommodate. In addition, the complexity of manufacturing and its costs are reduced.

One significant disadvantage of using single sensor pressure probes has been the increase in the running costs compared with multi-sensor pressure probes. Recently, Dambach and Hodson [3] proposed a new method of data reduction, based on the method of least squares, which means that the use of a single sensor pressure probe has become more attractive.

Dambach and Hodson used a single sensor pressure probe that was essentially a wedge probe with a sensor inserted into one of the faces. It was used to measure a flow field that was mainly 2D. The probe was designed to have only yaw sensitivity. However, the pitch sensitivity is also important in the survey of three dimensional turbomachinery flows. For single sensor pressure probes, the shape of a probe plays a very important role in its sensitivity because there is only one sensor. Therefore, an understanding of the flow around the probe and the ability to alter this flow by altering the shape of the probe are needed if the sensitivity of the probe to changes in the pitch angle is to be acceptable.

This paper presents the results of three sets of experiments. The steady state and dynamic behaviour are investigated in the first and second set. In the third series, selected probes are used to measure an unsteady flow.

2 Steady state large-scale model tests

In order to investigate the dependency of pitch and yaw sensitivity on probe shape, the performance of large-scale models has been investigated in a wind tunnel. Ten models were tested. All of the geometries were based on a simple shape. They are shown in Fig. 1. The pressure distribution on the sensing face of each model was measured. In addition, some flow visualization experiments were conducted in a smoke tunnel.

The nominal width (or diameter) of each model is 30mm, which is more than fifteen times larger than a real miniature probe. The probes are intended for use in inter-bladerow measurements. The probe stem is to be inserted radially into the machine. All the probes have the sensing face at the end of this radially mounted stem so that they can be rotated about the access of the stem. The main

geometric parameters that influence pitch sensitivity of the probe are

(1) the shape of the probe stem (e.g., Square, Circular, and Triangular) and
(2) the angle of the slanted sensing face of the probe tip

and the shapes of the probes have been chosen with these factors in mind.

2.1 Experimental setup

For the purposes of calibration, the model probes were positioned at the exit of a wind tunnel. The ratio of the hydraulic diameter of this exit to the width of each probe is about thirty, which is large enough to ensure that the flow can be regarded as a uniform freestream. Stepping motors were employed to change the yaw and pitch angles of the probes, whilst keeping the probe head at the centre of the wind tunnel. The definitions of the pitch angle and yaw angle are shown in Fig. 2.

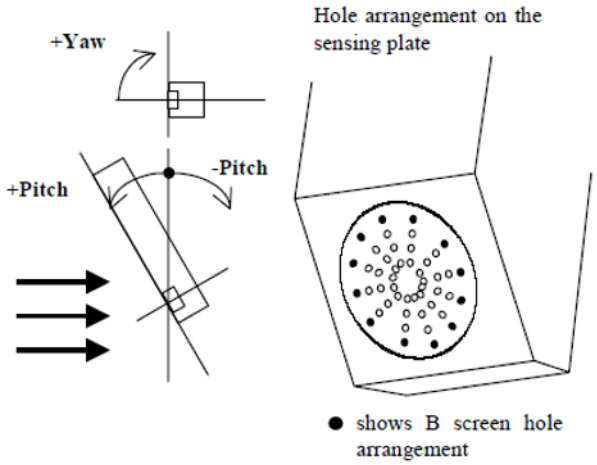

Fig. 2. Definition of pitch and yaw angle

To measure the steady state pressure distribution on the sensing face, a plate with the diameter of 20mm was used. The circular plate represents the face of a single pressure sensor. The plate was fitted with 48 pressure tappings as shown in Fig. 2. The pressures associated with each of the 48 pressure tappings on the sensing face and the static pressure and the dynamic pressure of the flow were automatically measured at each yaw-pitch position. In this way, the distribution of the static pressure coefficient C_p on the sensing plate was obtained at each angular position of the probe. An example of this is shown in Fig. 3.

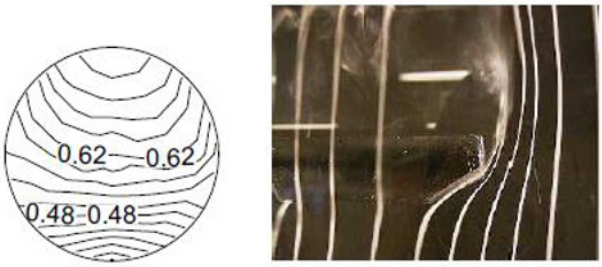

Fig. 3. Flow around a probe (right) and C_p distribution on the sensing plate (left) (Probe No.8 at α=β=0)

Commercially available miniature pressure sensors are sometimes provided with a screen that protects the active surface of the probe. In the case of Kulite pressure sensors, two types of screen are available. The B-type screen has 12 holes arranged around a circle close to the outer diameter. In this paper, the data obtained on a circle close to the outer diameter of the plate (see Fig. 2) was averaged to produce a pressure that is a representative of that which would be measured by a sensor fitted with this type of screen. This assumes that the pressure on the actual sensor would be the average of the pressure of each hole in the screen. Furthermore, it is believed that of this type of arrangement represents the greatest challenge in terms of achieving a good pitch sensitivity.

2.2 Experimental conditions

The experimental conditions are shown in Table 1. The diameters d of the single sensor probes employed for fast response measurements in turbomachines are expected to be of the order of 1 mm to 2 mm and the freestream velocities V will range from about 100 to 300 m/s. Using these values and ambient values for the properties of air gives Reynolds numbers in the range

$$10{,}000 \leq Re = \frac{Vd}{v} \leq 120{,}000$$

In the experiments reported in this paper, the freestream velocity was set to either 20 or 40 m/s for the model probes, which had a nominal diameter of 30 mm. This gave a Reynolds number of 40,000 or 80,000 respectively, which includes the most important part of the range to be found in actual use.

Table 1. Experimental conditions

	CASE 1	CASE 2
	Basic Condition	Re dependency test
Velocity (m/s)	20	40
Yaw angle (deg)	0 to 360, every 18 deg	
Pitch angle (deg)	-60 to 60, every 15 deg	
Reynolds Number	40,000	80,000
Probe Model	All models	Only Probe No. 1

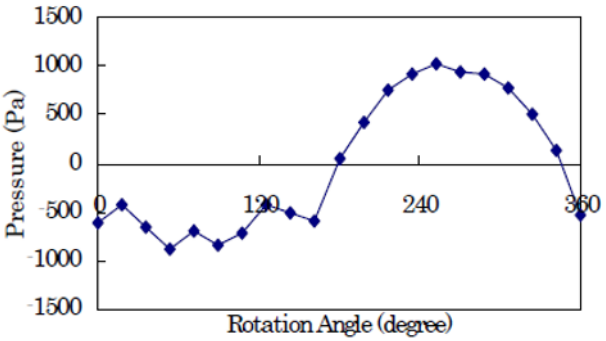

Fig. 4. A sample of measured data

2.3 The "least squares method" of the data reduction

When using a single sensor pressure probe for the measurement of three-dimensional flows, there are 4 unknown parameters. They are the static pressure P_s, the stagnation pressure P_t, the yaw angle α and the pitch angle β. In a real measurement, the probe would be inserted into the flow and then rotated around the axis of its stem so that the pressure on the sensor could be measured at a

number of angular (i.e., yaw) positions. A graph of the measured pressure at each angular position might resemble that shown in Fig. 4. As yet, the static pressure, the stagnation pressure, the yaw angle and the pitch angle are unknown.

The calibration data of a typical probe is shown in Fig. 5. It can be seen that the shape of the variation of the static pressure coefficient

$$C_p(\alpha,\beta) = \frac{P(\alpha,\beta) - P_s}{P_t - P_s}$$

with yaw angle depends on the pitch angle. By comparing data such as that shown in Fig. 4 with the calibration data such as that shown in Fig. 5, it is possible to determine the unknown parameters. Formally, this comparison is carried out using the least squares method that aims to minimize the quantity

$$\langle \chi^2 \rangle = \sum_{i=1}^{N} \Big(P_i - \big((P_t - P_s) C_p(\alpha,\beta) + P_s \big) \Big)$$

where the summation is carried out over the number N of angular positions of the probe.

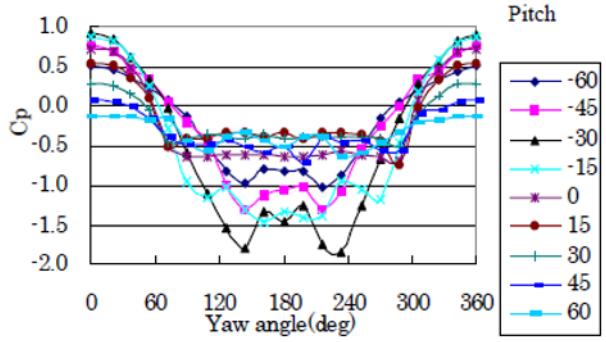

Fig. 5. A sample of calibration data

2.4 The definition of "Pitch sensitivity" for a single-sensor pressure probe

The shape of the curve shown in fig. 4 shows that the sensitivity of the sample probe to changes in yaw angle is more than adequate. This is primarily because, in use, the probe will be rotated about the axis of the radial stem over a large range of angles. Unfortunately, the pitch of the probe cannot be changed while it is being used to make measurements. Therefore, the data reduction technique essentially relies on the fact that the sensitivity of the probe to changes in yaw angle depends on the pitch angle. In effect, during the processing of the data using the least squares method, the matching of a measured curve such as that shown in Fig. 4 to the calibration data involves the horizontal and vertical position and the vertical scale being altered so that the measured curve overlays the calibration data at the appropriate pitch angle as close as is possible. The horizontal shift gives the yaw angle, the vertical shift gives the static pressure and the vertical scaling provides the dynamic pressure. More importantly, the variation with pitch angle of the "Shape" of calibration curves such as those shown in Fig. 5 defines the "pitch sensitivity".

In this paper, only the data obtained at yaw angles from 0 to 72 and from 288 to 360 degrees were used to determine the pitch sensitivity. This range was chosen in order to reduce the dependency of the sensitivity on the separated flow behaviour of the probe. This is because the separated flow behaviour is often strongly dependent on Reynolds Number. It may also be altered by unsteadiness in the freestream. In fact, the use of other ranges of angle, such as from 0 to 90 and from 270 to 360 degrees were considered. However, a careful investigation of the results revealed that the former range is to be preferred. This seems reasonable because the flow around a cylinder begins to separate at about 83 degrees. In use, data obtained from outside the same restricted range of yaw angles will also be rejected for the same reasons. Thus, not only the aerodynamic shape of a probe, but also the data processing algorithm is important in ensuring the quality of the data obtained using a single sensor pressure probe.

Given that of the shape of the calibration curves such as those shown in Fig. 5 defines the pitch sensitivity, the pitch sensitivity has been defined in the following way. A new parameter

$$C_p^*(\alpha,\beta) = \frac{C_p(\alpha,\beta) - C_p(\alpha_1,\beta)}{C_p(0,\beta) - C_p(\alpha_1,\beta)} = \frac{P(\alpha,\beta) - P(\alpha_1,\beta)}{P(0,\beta) - P(\alpha_1,\beta)}$$

is used as the basis of the assessment of pitch sensitivity. Here, α_1 is equal to 72 degrees for the reasons mentioned above. The

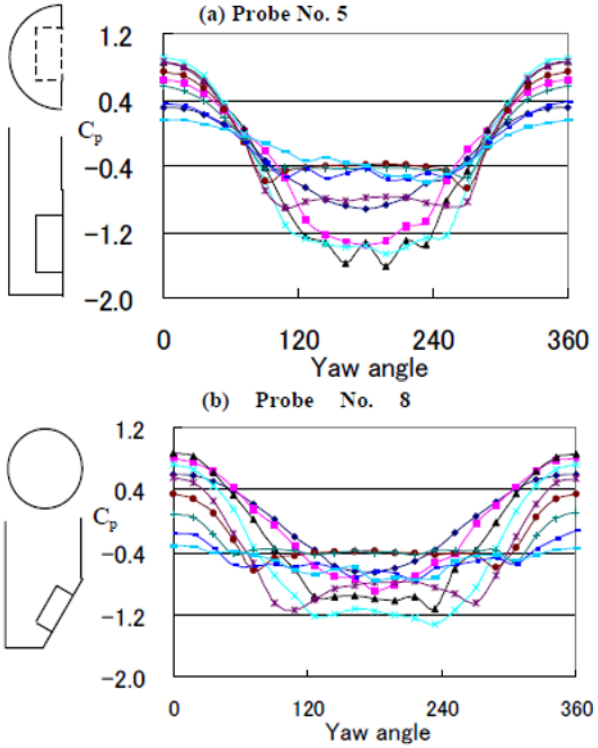

Fig. 6. C_p vs yaw angle (for key see Fig. 5.) for two designs of cylindrical probe

sensitivity $S(\beta_1,\beta_2)$ between two pitch angles β_1 and β_2 where $\beta_1 \geq \beta_2$ is then expressed as

$$S(\beta_1,\beta_2) = Min\langle \lambda^2 \rangle$$

Where

$$\lambda^2 = \int_{-\alpha_1}^{\alpha_1} \left[C_p^*(\alpha,\beta_1) - \{AC_p^*(\alpha,\beta_2) + B\}\right]^2 d\alpha$$

and A is a stretch factor and B is an offset. The quantities A and B are used because it is only the shape of the curves that are important. The new quantities A and B are obtained using the least squares method.

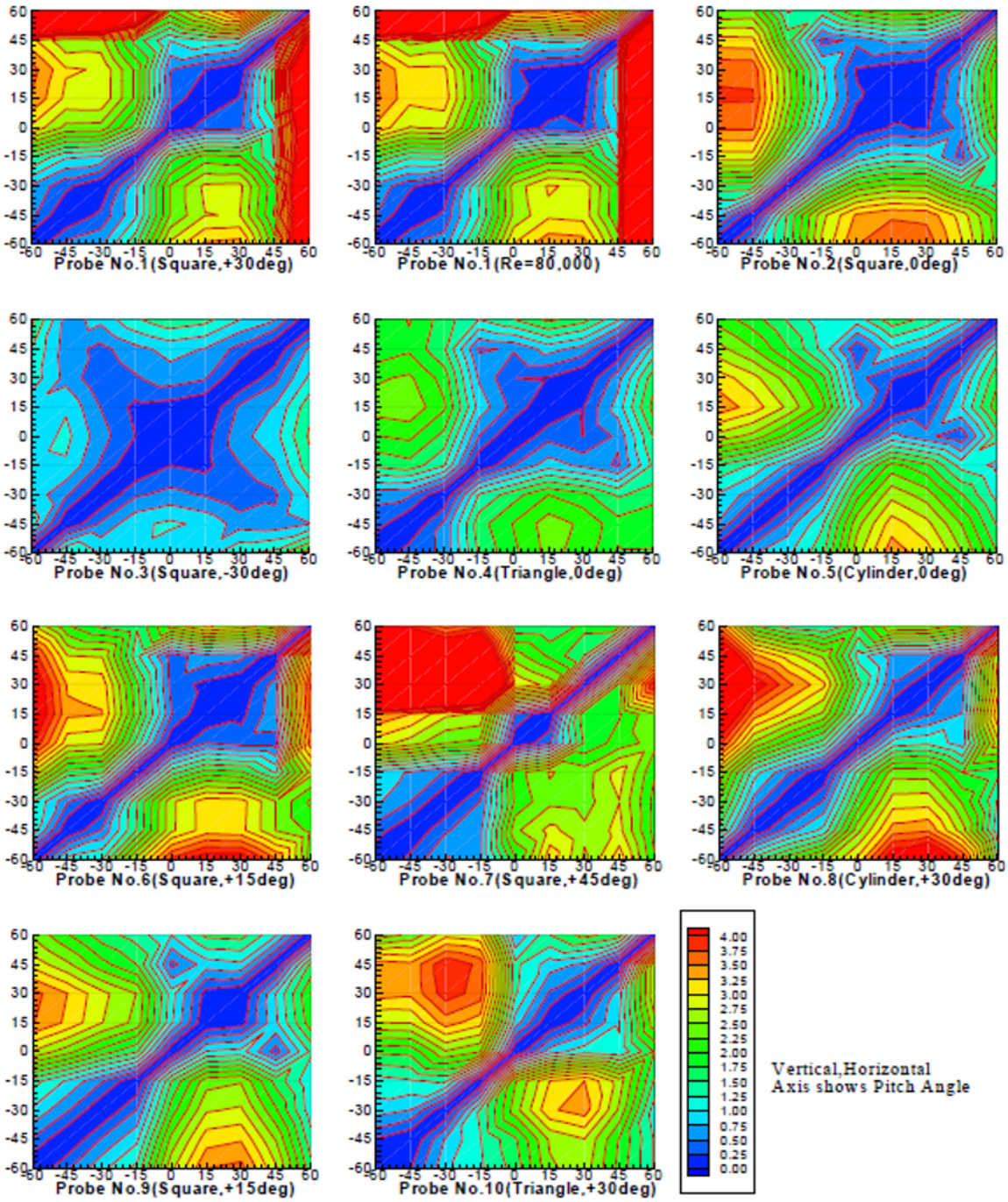

Fig. 7. Pitch sensitivity (Re = 40,000 except where stated)

2.5 Results

2.5.1 Effects of Slanted Face Angle on pitch sensitivity

Fig. 7 presents contours of the sensitivity $S(\beta_1,\beta_2)$, as defined above, for the 10 probes shown in Fig. 1. The pitch angle is both the ordinate and the abscissa. Note that as a result of the definition used

$$S(\beta_1,\beta_2) = S(\beta_2,\beta_1)$$

The results for the square type probes (No.s 1, 2, 3, 6 and 7) indicate that increasing the slanted face angle of the probe increases the pitch sensitivity. Examination of the contour maps shows that, for example, probe No. 1 (slanted face angle = +30 deg) seems best. This is because the sensitivity is high over most of the diagram, except along the diagonal where it must be zero since $\beta_1 = \beta_2$. Probe No. 3 (-30 deg) has almost no sensitivity to pitch. Probe No. 7 (+45 deg) also has a reasonable performance but only at pitch angles between 0 and 30. Below this pitch angle, the sensitivity is not good enough. Above this,

the sensitivity is essentially zero. Probe No. 2 (0 deg) is unsatisfactory at positive pitch angles.

Fig. 6 presents the calibration curves for two of the cylindrical probes. It shows how the pressure coefficient varies with yaw angle at each of the pitch angles of Fig. 5. In the case of Probe No. 5 (Fig. 6(a)), all the curves converge at yaw angles of about 70 degrees and 290 degrees. In this case, the shape of each curve is similar to the others. This means that there is less sensitivity. In the case of Probe No. 8 (Fig. 6(b)), which has a slanted face angle of 30 degrees, the shape of each curve is very different at yaw angles less than 70 degrees or greater than 290 degrees. These changes in shape are reflected in the values of the sensitivity coefficient plotted in Fig. 7.

In the case of the cylindrical probes, Fig. 7 shows that Probe No. 8 (+30 deg) has a better sensitivity than Probe No. 5 (+0 deg) or Probe No. 9 (+15deg). In the case of the triangular probes, Probe No. 10 (+30 deg) has better sensitivity than Probe No. 4 (+0deg). Thus it can be seen that increasing the slanted face angle increases the pitch sensitivity and the best slanted face angle is +30 degrees, regardless of probe type.

Comparing sensitivity contour of the +30 deg slanted face designs with each other (No. 1 with No. 8 and No. 10), probe No. 8 and probe No. 10 seem to have good sensitivity at high pitch angles. Furthermore probe No. 1 and No. 8 seem to have good sensitivity at low (negative) pitch angles. Thus, probe No. 8 seems to have the best sensitivity over a wide range of pitch angles.

In summary, the present results indicate that the best probe design is Probe No. 8 (cylindrical; +30 deg).

2.5.2 Effects of Reynolds Number on pitch sensitivity

For the range of Reynolds numbers under investigation here, Fig 7 indicates that there does not seem to be any dependency on the Reynolds number in the case of probe No. 1 (+30 deg). This is revealed by comparing the left-hand and central plots at the top of the figure. This is a typical result.

3 Dynamic large-scale model test (angularly fluctuating flow)

In the flow downstream of the rotor blades of a turbine or compressor, not only the velocity but also the flow angle fluctuates as the wakes and secondary flow features pass by the stationary observer. In this experiment, in order to investigate the dynamic effect of angular fluctuations of the flow, a probe was mounted on a crank mechanism that was driven by a motor. The crank mechanism causes the probe yaw angle to oscillate in the flow, as opposed to changing the angle of the flow. Probe No. 1 and No. 8 were selected for these experiments.

3.1 Experimental Setup

Fig. 8 shows the driving mechanism which creates the angular oscillation of the probes at the outlet of the wind tunnel.

The crank mechanism can generate oscillations up to a maximum frequency of 50 Hz with an amplitude of between 10 and 30 degrees.

A 16 channel Scanivalve DSA system was used to capture the unsteady pressure signals. The sensing face of the probe was fitted with a sensing plate similar to that used in the steady state measurements. In this case, there are 13 pressure tappings on the sensing plate that are connected to Scanivalve DSA using flexible tubes which are about 400 mm in length. The length of the tubes was designed to keep the propagation delay and the attenuation of the signal to a minimum. The propagation delay and the attenuation was measured by comparing the data obtained using the DSA system with that obtained using a Kulite XCS062 pressure transducer that was fitted in place of one of the pressure tappings. The delay was found to be 2.3 ms. There was no appreciable attenuation. The data were acquired at a frequency of 200 Hz per channel. All of the data acquisition was phase-locked with respect to a trigger signal from the rotating disk of crank mechanism. The oscillation frequency was chosen in order to avoid mechanical resonances of the system.

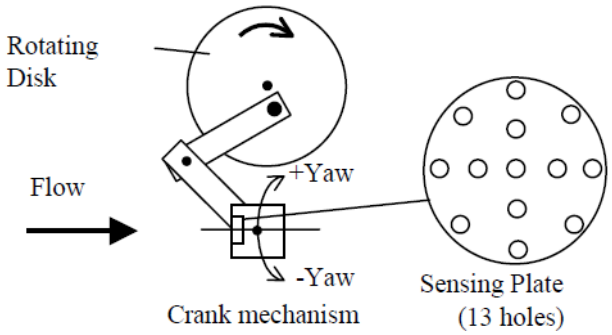

Fig. 8. Experimental setup

3.2 Experimental Conditions

In turbomachines, with the fundamental frequency *f* of the flow fluctuations being identical to the blade-passing frequency, and with freestream velocities u_∞ ranging from 100 to 300m/s, the governing non dimensional parameter, i.e., the Strouhal Number, for dynamic flows is of the order

$$St = \frac{fd}{u_\infty} = 0.01 \ldots 0.15$$

The maximum frequency of oscillation in the present experiment is 50 Hz and the minimum freestream velocity is 10m/s if the sensitivity of the pressure transducer is taken into account. Thus the maximum Strouhal Number is set at 0.15 in the experiment. In fact, relatively large amounts of hysteresis have been observed at lower Strouhal Numbers, which indicates that this condition was sufficient for the purposes of observing the dynamic effects. The test conditions reported here are given in table 2.

Table 2. Experimental conditions

		Probe No2		Probe No8	
Case	(a)	(b)	(c)	(d)	(e)
Velocity (m/s)	20	15	15	20	15
Frequency (Hz)	16.7	12.5	25	16.7	25
Amplitude	20 deg	20 deg	20 deg	20 deg	20 deg
St	0.025	0.025	0.05	0.025	0.05

3.3 Results

Fig. 9(a) to Fig. 9(e) present a summary of the results of these unsteady experiments. Each graph shows the variation of Cp with yaw angle for one period of oscillation. All the data are phase-lock averaged. Not only the averaged Cp of the B-type screen hole arrangement (labelled outer holes), but also the value of Cp at centre hole are shown. The results from the steady state experiments are also shown. If there is no hysteresis, all the plots should coincide with steady state results. The differences between the steady state and unsteady results is due to the dynamic effects.

In the case of probe No. 2, comparing Fig. 9(a) with Fig. 9(c) shows that the hysteresis loop becomes larger as the Strouhal number is increased. The same thing is not observed in the case of probe No. 8. (compare Fig. 9(d) and Fig. 9(e)).

Comparing Fig. 9(a) with Fig. 9(b), shows that they are quite similar to each other even though the frequencies of oscillation are different. This implies that the Strouhal Number is the parameter of interest in an angularly fluctuating flow field. Comparing Fig. 9(a) with Fig. 9(d) shows that the cylindrical probe (No. 8) has a much smaller hysteresis loop than square probe (No. 2). The flow visualisation experiments showed that this is because the separation lines on the cylindrical probe stem do not alter their position in absolute space even if the probe rotates. In the case of the square probe, the separation point moves as the probe rotates around its axis because the corners of the square section always define the starting point of separation. If the separation point moves, the pressure potential field around the probe changes considerably. Since the dynamic behaviour of separated flow can be very different to that observed in steady flow, the pressures acting on the sensing plate of the probe are affected by the dynamic phenomena of separation. This tendency becomes larger as the Strouhal Number increases. Within the range of the experiment, it is concluded that a cylindrical type tends to be less affected by dynamic effects than a square type. Thus the best probe is cylindrical type because it is less affected by dynamic phenomena.

It is concluded that the best probe is probe No. 8. This conclusion is based on both the steady state and the dynamic experiments.

4 Application of the least squares method to unsteady flow measurement

In the experiments described here, a moving bar rig was employed as a wake generator to create a flow in which the velocity fluctuates in both angle and magnitude. Selected model probes were employed to measure the unsteady flow which results from traversing a cylindrical bar across the flow upstream of the probes. The least squares method was used to process the acquired data. In this way, the feasibility of using the selected probes for the measurement of unsteady flow field was examined.

4.1 Experimental Setup

Fig. 10 shows the general view of the moving bar rig. A largescale probe is mounted at the outlet of the wind tunnel. The
cylindrical bars traverse the flow from top to bottom and can

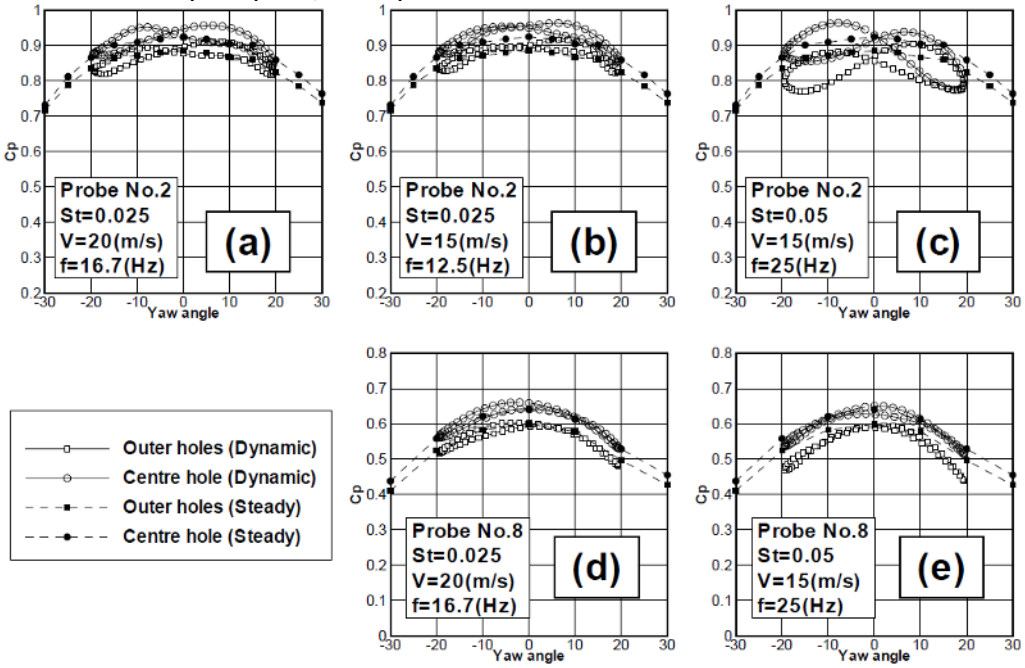

Fig. 9. Correlation between C_p and yaw angle in one period of oscillation

generate unsteady wakes up to a passing frequency of 15 Hz.

In turbomachines, the width of trailing edge of a blade is of a comparable order of magnitude to a real miniature probe, the size of which is expected to be less than 2 mm. The large-scale models tested are 30 mm in size. Accordingly, moving bars with a diameter of 20mm were used in the experiment.

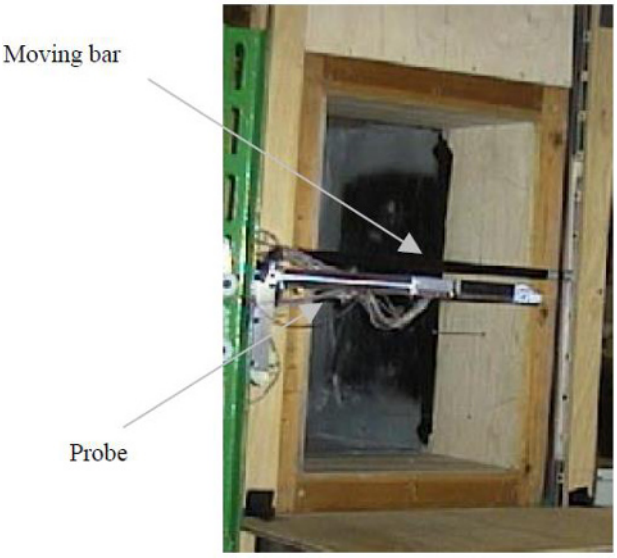

Fig. 10. Moving bar rig viewed looking upstream

Again, a Scanivalve DSA system was used for the high frequency data logging. Each bar generates a trigger signal when it passes through a certain point with respect to the probe. All the data was phase-locked in the data processing. Prior to using the large-scale models, a survey of the unsteady flow field was conducted using a hot-wire anemometer. A Dantec miniature hotwire, which was much smaller than the large-scale model probes, was placed perpendicular to the flow and parallel to the bars at a distance of 233mm from the plane of the moving bars. This was used to measure the fluctuations in the magnitude of the velocity.

4.2 Experimental Conditions

It has already been noted above that a large hysteresis was observed as a result of angular fluctuations in the flow at a relatively low Strouhal Number of about 0.025. In this experiment, the Strouhal Number was also set at about 0.025. Two conditions

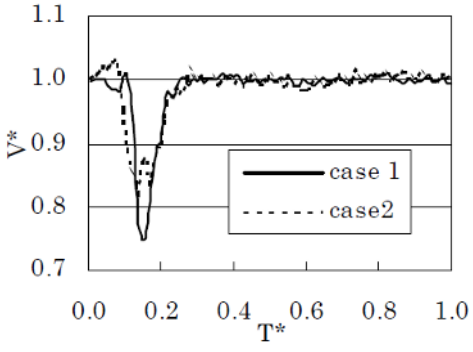

Fig. 11. Normalised velocity over 1 wake passing period measured using the hot-wire anemometer

were selected, corresponding to different wake passing frequencies as shown in Table 3.

Table 3. Experimental conditions

	CASE 1	CASE 2
Probe Size (m)	0.03	0.03
Freestream velocity (m/s)	20.4	10.2
Bar velocity (m/s)	10.6	6.14
Bar Passing Frequency(Hz)	14.7	8.5
Strouhal Number	0.022	0.025
Probe No. Tested	No. 1, No. 2, No. 8	

4.3 Results and Discussion

Comparisons of the results obtained using the model probes and the hot-wire are shown in Fig. 12. All the data were phase-locked with respect to moving bar. Here the least squares method was used to calculate the unknown parameters.

For all of the types of probe, case 2 is closer to hot-wire results than case 1. Comparing the results of velocity between hot-wire and probe model, they matches better at lower velocity than higher velocity although Strouhal number is almost the same. There are two possible reasons for this.

Kovasznay et. al [4] have shown that the inertial effects at the most upstream point of a sphere can be described as follows. Because this equation is derived for a sphere, strictly, it cannot be

$$P = P_o + \underbrace{\frac{1}{2}\rho V^2}_{\text{Dynamic Head Term}} + \underbrace{\frac{3}{8}\rho a \frac{dV}{dt}}_{\text{Inertial Term}} \qquad (a = \text{Diameter of sphere})$$

applied to the model probes tested here. However, the equation does show that the inertial effects would not be negligible when dV/dt or the probe size a is large. The probe size is large relative to the scale of the flow. Also, Fig. 11 shows that the relative magnitude of the velocity perturbation is greater and the width is less for Case 1 in comparison to Case 2. As a consequence, the effect of the inertial term (i.e. dV/dt) becomes larger.

According to the results from the hot-wire measurements, the wake width is larger in case 2 than in case 1 (see Fig. 12). In Case 1, the width of the wake is approximately 135 mm at the measurement location. It is approximately 160 mm in Case 2. The probes have a width of 30 mm. These differences and the fact that the probe, though smaller, is of a similar order of magnitude to the wake, which means that the agreement between the hot-wire measurements and those of the probe is better in Case 2 since there is less "smearing" of the data. This result shows that the relative size of the probe is important in determining the quality of the unsteady measurements.

Overall, no significant difference was found between the measurement accuracy of the probes tested here. This means either that no probe has an advantage over the others in terms of the dynamic effects when the magnitude of the flow varies or that the Strouhal Number is not large enough to produce any differences. In general, the velocity indicated by the model probes is in good

agreement with that indicated by the hot-wire measurements. Thus, the least squares method for data processing was successfully applied to the measurement of unsteady flow behind a moving bar.

5 Conclusions

Ten types of probe were designed and tested in a wind tunnel in order to investigate the effect of the shape of a probe on its yaw and pitch sensitivity. By using large scale model testing, it was found that using a slanted sensor face increased the pitch sensitivity of a single sensor pressure probe. A dynamic test was conducted for a few selected probes on the basis of the steady state results. In an angular fluctuating flow, a large hysteresis was observed for square type probes at relatively low Strouhal Numbers. It was found that cylindrical probe design tended to be less affected than square probe within the range of flow conditions tested. In a second set of unsteady measurements, carried out behind a moving bar and where the flow is fluctuating mainly in magnitude, there is no difference observed among model probes tested. Finally the least squares method of data processing for a single sensor pressure probe model was successfully applied in the measurement of unsteady flow.

References

1. L. R. Bissonnette, S. L. Mellor, *Experiments on the Behaviour of an Axisymmetric Turbulent Boundary Layer with a Sudden Circumferential Strain*, J. Fluid Much., **63**, pt 2 (1974)
2. M. A. Cherret, J. D. Bryce, H. P. Hodson, *Development of pneumatic probes for measurements in 2-D and 3-D flows*, 12th Symp.. on Measuring Techniques for Transonic and Supersonic Flow in Cascades and Turbomachines, Munich, Sept. (1992)
3. R. Dambach, H. P. Hodson, *Single-Sensor Fast Response Pressure Probes – The "Least Squares" Method of Data Reduction*, 15th Symp. on Measuring Techniques for Transonic and Supersonic Flow in Cascades and Turbomachines (1998)
4. H. Fujita, L. S. H. Kovasznay, *Measurement of Reynolds Stress by a Single Rotated Hot wire Anemometer*, Rev. Sci. Instrum., **39**, pp 1351-1355 (1968)
5. A. Goto, *Three dimensional flow and mixing in an axial flow compressor with different rotor tip clearances*, ASME Paper 91-GT-89, June (1991)
6. C. R. Grossweiler, H. J. Humm, P. Kupferschmeid, *The use of piezo resistive semi-conductor pressure transducers for fast response probe measurements in turbomachinery*, 10th Symp.. on Measuring Techniques for Transonic and Supersonic Flow in Cascades and Turbomachines, Brussels, Sept. (1990)
7. H. J. Humm, C. R. Grossweiler, G. Gyamarthy, *On fast-response pressure probes: Part 2 – Aerodynamic probe design studies*,J. Turbomach. Trans. ASME, **117**, pp 618-624, Oct. (1995)
8. P. Kool, *Determination of the Reynolds Stress Tensor with a Single Slanted Hot wire in Periodically Unsteady Turbomachinery Flow*, ASME paper 79-GT-130, March. (1979)
9. L. S. G. Kovasznay, I. Tani, M. Kawamura, H. Fujita, *Instantaneous Pressure Distribution Around a Sphere in Unsteady Flow*, J. Fluids Eng. **103** (1981)
10. M. Kuroumaru, M. Inoue, T. Higki, FA-E Abd-Elkhalek, T. Ikui, *Measurement of Three Dimensional Flow Field behind and Impeller by means of Periodic Multi-Sampling with a Slanted Hot wire*, Bulletin of JSME, **25**, No. 209, Nov. (1982)
11. J. T. McGuire, J. P. Gostelow, *Experimental Determination of Centrifugal Impeller Discharge Flow and Slip Factor*, ASME paper 85-GT-77 (1985)
12. D. B. Sims-Williams, *The initial development of a pressure probe for active measurement of unsteady flows*, University of Cambridge, Dept. of Engineering, Final Year Project Report (1994).
13. C. E. Whitfield, J. C. Kelly, B. Barry, *A three-dimensional analysis of rotor wakes*, Aero. Quart., Nov. , pp 285-300 (1972)

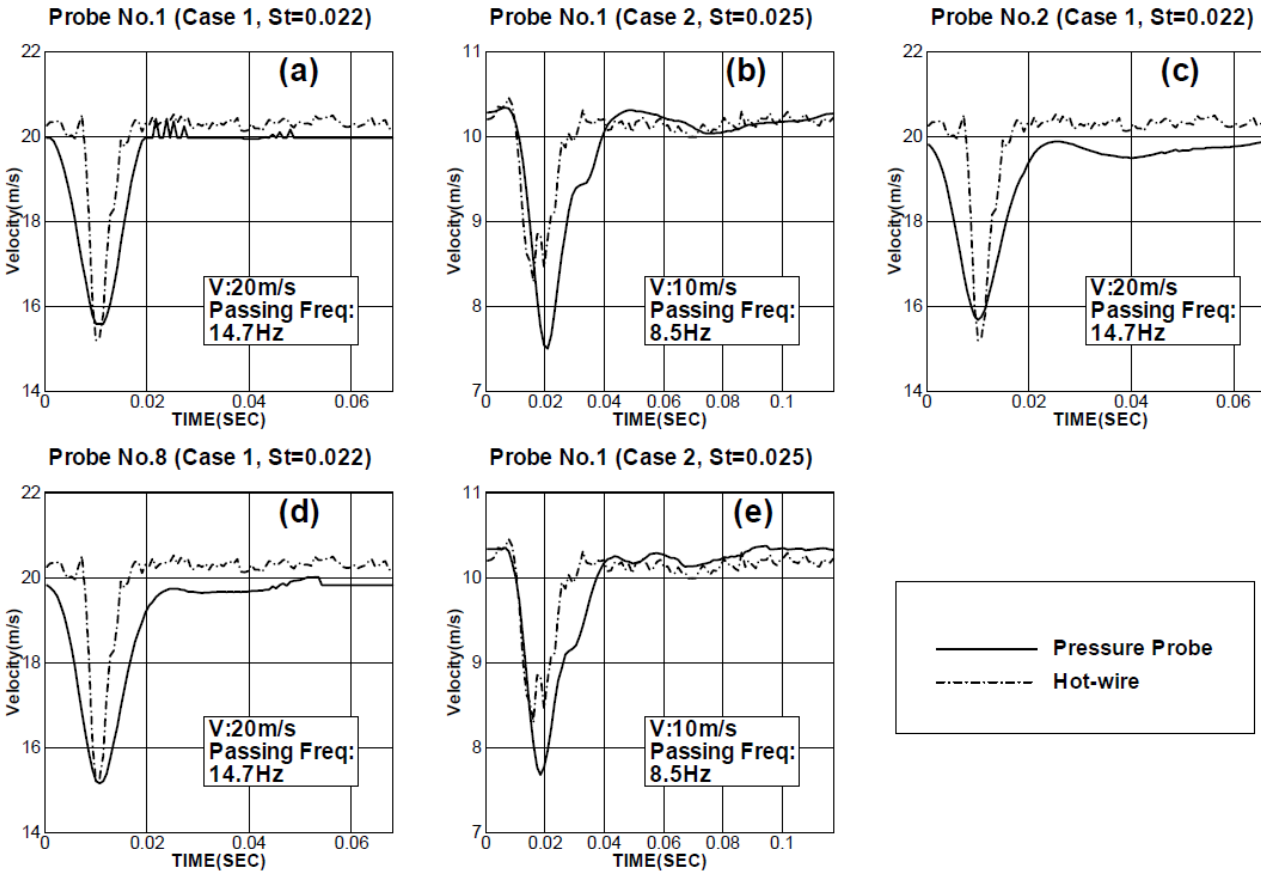

Fig. 12. Comparison of results between Pressure Probe and Hot-wire (phase-locked, 1 wake passing period shown)